

Acoustics of a Helmholtz Resonator Aligned Parallel with Flow: A Computational Study VS. Experiments

Emel Selamet, Ahmet Selamet, Asim Iqbal, and Hyunsu Kim

Abstract—Acoustic attenuation of a Helmholtz resonator (HR) placed parallel to the flow path is investigated computationally with and without mean flow and compared with experimental results. The time-dependent flow field is determined by solving three-dimensional unsteady, laminar/turbulent, compressible Navier-Stokes equations using Pressure-Implicit-Splitting-of-Operators algorithm of STAR-CD. Computations are performed by different finite difference schemes such as central and upwind for momentum equation. Predictions with central differencing, a blending (with upwind) factor 0.5, and fine mesh reveal results that are consistent with the experimental observations. The effect of flow on the acoustic attenuation characteristics of HR has been illustrated both computationally and experimentally. The predictions for transmission loss exhibit reduced attenuation at elevated flow rates.

Index Terms—Helmholtz resonator, flow effect on acoustics, transmission loss.

I. INTRODUCTION

A variety of analytical, computational, and experimental studies is available in literature to investigate the acoustic behaviour of HRs since they are extensively used in many applications, such as the breathing system of internal combustion engines and compressors [1]-[3]. One of the critical factors influencing their acoustic performance is the presence of mean flow. A recent study [4], for example, examines this effect for a HR with its neck oriented perpendicular to flow. The emphasis of the present study remains the flow effect as applied, however, to a different orientation of a ("charged") HR, where the silencer of [4] is now aligned parallel to the incident flow as illustrated in Fig. 1. Multidimensional time domain computations are performed to predict the acoustic behaviour of this HR. These predictions are then compared with experimental results on a flow-impedance tube setup, which is described in [4]. In the setup, pressure transducers are located at two upstream (referred to as locations 1 and 2 hereafter) and two downstream locations (3 and 4), 4 cm apart from each other, for capturing the pressure fluctuations which are then used to calculate the acoustic attenuation in terms of transmission loss.

Following this Introduction, Section II briefly describes the solution method. Computational results and their comparison with experimental data are presented in Section III, followed by concluding remarks in Section IV.

Manuscript received January 15, 2013; revised February 26, 2013.

Emel Selamet, Ahmet Selamet, Asim Iqbal, and Hyunsu Kim are with the Center for Automotive Research, The Ohio State University, Columbus, OH, 43210, USA, (e-mail: Selamet.2@osu.edu; Selamet.1@osu.edu; iqbal.27@osu.edu; kim.2287@osu.edu).



Fig. 1. Surface mesh of the system.

II. SOLUTION METHOD

Compressible air flow in ducts is simulated by STAR-CD which combines Pressure-Implicit-Splitting-of-Operators (PISO) algorithm for transient flows with the fully-implicit Euler and explicit deferred correctors [5]. For the solution of discretized conservation of momentum, mass, and energy equations a blending factor is introduced which can vary from 0 to 1. Blending factor defines the level of upwind differencing incorporated in the discretization. The computational domain is initially set to stagnant (zero velocity) conditions at $p = 101 \text{ kPa}$ and $T = 293 \text{ K}$. The boundary conditions at the inlet and outlet are given as follows. At the inlet

$$u_{\text{inlet}} = u_m + 0.01 \sin(\omega t) \quad (1)$$

where u_m is the mean velocity and $\omega (= 2 \pi f)$ the angular frequency. For the outlet, transient-wave transmissive boundary is selected among built-in boundary condition selections. This condition allows transient waves to exit the domain without any reflection, hence providing an anechoic termination.

The mesh is composed of 83691 vertices and 71245 cells (coarse mesh) for the inlet and outlet duct lengths of 84.5 cm. The lengths of cylindrical resonator cavity and neck are 24.4 cm and 8 cm, while their radii are 7.5 cm and 2 cm, respectively. The results are also obtained with finer mesh and with the inlet and outlet duct lengths of 60.3 cm which resulted in 147336 vertices and 81955 cells. Shortening the duct lengths reduces the cpu time, while improving the resolution.

III. RESULTS AND DISCUSSION

Simulations are carried out for $u_{\text{inlet}} = 0.0, 17.15, \text{ and } 34 \text{ m/s}$, $\text{Ma} = 0, 0.05, \text{ and } 0.1$, respectively. The runs are terminated when the residuals of momentum, mass, and energy stay within a certain interval and do not decrease

any further indicating that a pseudo steady state is reached in the computational domain. The histories of fluctuating pressures at the inlet and outlet locations are obtained for different velocities and frequencies so that the acoustic performance properties such as the transmission loss can be predicted. Fast Fourier transform (FFT) of the temporal data provides the pertinent frequency domain information. The frequency spectrum reveals the resonance (or, the dominant) frequency. Sound pressure level (SPL) is a logarithmic measure of the sound pressure expressed as

$$SPL = 20 \log_{10} \frac{P_{rms}}{P_{ref}} \text{ in dB,}$$

where p_{rms} is the rms sound pressure and $p_{ref} = 20 \mu\text{Pascals}$. Transmission loss (TL) is related to the reduction of SPL in transmitted wave relative to incident wave as the sound travels through a component. The two-microphone technique [6], [7] is applied under the condition of equal cross-sectional areas at the inlet and outlet locations. It gives, by using FFT of the fluctuating pressures at locations 1 through 4,

$$TL = 10 \log_{10} \frac{P_1(f)e^{ik_r s} - P_2(f)}{P_3(f)e^{ik_r s} - P_4(f)},$$

where s is the distance between two microphones (or corresponding pressure pickup locations in simulations), k_r the wave number of the reflected pressure and defined as $k/(1 - Ma)$.

A. Effect of Blending Factor

First, the simulations are performed for $Ma=0.05$ with a coarse mesh. It is observed that for the spatial central differencing with different blending factors (BF) yield different results. Fig. 2 depicts the transmission loss for $Ma=0.05$ obtained with central differencing scheme which employs blending factors of 0.2, 0.5, and 0.8 for the solution of momentum equation. Since the predictions match the experimental results reasonably well with $BF=0.5$, the remainder of the runs in the present study are performed with this value.

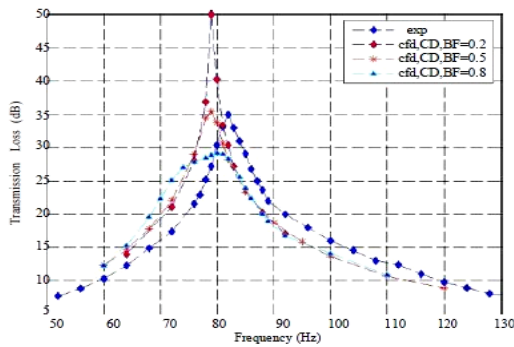


Fig. 2. Transmission Loss versus frequency for $Ma=0.05$ with different blending factors.

B. Zero Mean Flow Results ($Ma=0.0$)

Fig. 3 compares the predicted and experimental transmission losses with $L_{duct} = 84.5 \text{ cm}$ and coarse mesh. The predicted TL values are shifted slightly to the left and

peak TL is slightly overestimated. This case is repeated with smaller mesh size but shorter length (60.3 cm) to improve the resolution with the corresponding results presented in Fig. 4. While the predicted peak TL is still slightly overestimated, overall predicted and experimental results agree very well in the frequency range of 60-120 Hz, hence the shift has been eliminated thanks to the improved resolution.

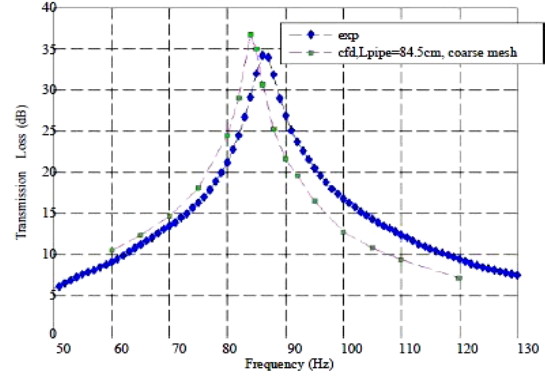


Fig. 3. Transmission Loss versus frequency for $Ma=0.0$ with $L_{pipe} = 84.5 \text{ cm}$ and coarse mesh.

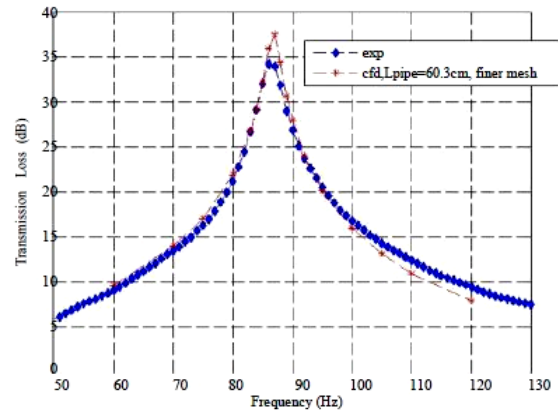


Fig. 4. Transmission Loss versus frequency for $Ma=0.0$ with $L_{pipe} = 60.3 \text{ cm}$ and finer mesh.

C. Mean velocity of 17.15m/s ($Ma=0.05$)

Fig. 5 compares the predicted and experimental transmission losses with $L_{duct} = 84.5 \text{ cm}$. Again, the predicted TL curve is shifted slightly to the left. Similarly, when this case is re-examined with reduced mesh size and shorter length (60.3 cm), a good agreement is obtained between the predictions and experiments, as illustrated in Fig. 6. Note that the peak TL magnitude with $Ma=0.05$ has not yet changed noticeably relative to the no-flow case.

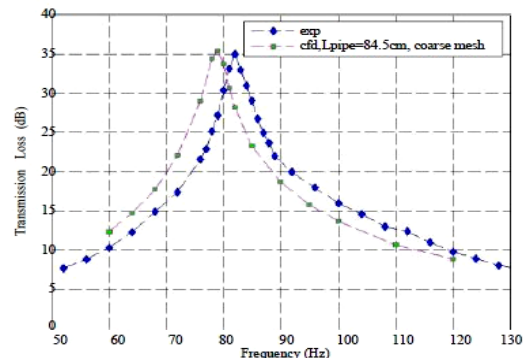


Fig. 5. Transmission Loss versus frequency for $Ma=0.05$ with $L_{pipe} = 84.5 \text{ cm}$ and coarse mesh.

D. Mean Velocity of 34 m/s ($Ma=0.1$)

TL for this case is presented only for finer mesh with $L_{duct} = 60.3 \text{ cm}$. The comparison of the predicted and experimental TL in Fig. 7 reveals a relatively reasonable agreement. Since the flow rate is higher for this case, reducing the mesh size further may improve the results. While the maximum values of TL with $Ma=0$ and 0.05 were approximately the same (about 35 dB), it has now dropped dramatically to about 16 dB for $Ma=0.1$. This may possibly be attributed to the fact that the fluid residence time, hence the ability to interact with the resonator, is reduced with increasing velocity. Therefore, it is necessary to take the effect of mean flow into account for predicting accurately the acoustic performance of a system with Helmholtz resonators.

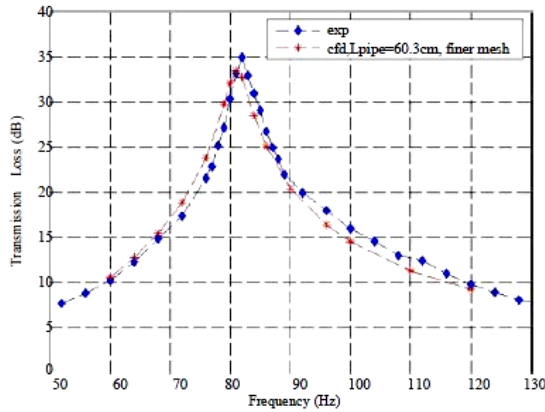


Fig. 6. Transmission Loss versus frequency for $Ma=0.05$ with $L_{pipe} = 60.3 \text{ cm}$ and finer mesh.

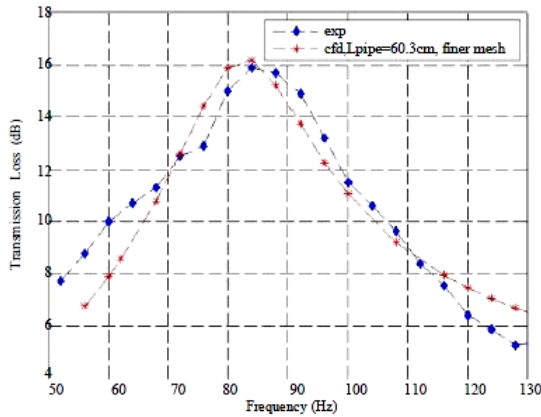


Fig. 7. Transmission Loss versus frequency for $Ma=0.1$ with $L_{pipe} = 60.3 \text{ cm}$ and finer mesh.

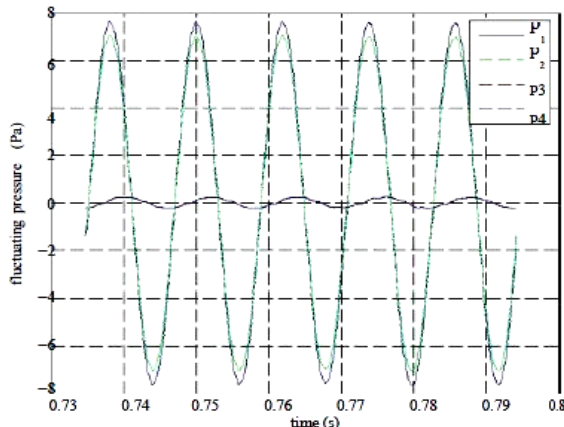


Fig. 8. Pressure fluctuations at location 1, 2, 3 and 4 for $u_{in}=17 \text{ m/s}$ at $f=84 \text{ Hz}$ with HR.

E. Acoustic Pressures

To examine the acoustic pressure variation in the present configuration with HR, an example case of $Ma=0.05$ and $f=84 \text{ Hz}$ is considered. To isolate the effect of HR on the system, acoustic pressures are also computed with the same ducts but without HR. Fig. 8 shows the fluctuating pressures at locations 1, 2 (inlet), 3, and 4 (outlet) with the HR, whereas Fig. 9 shows the same quantities without HR. The comparison of p_3 and p_4 in Figs. 8 and 9 clearly illustrates that the acoustic pressures at the outlet are dramatically suppressed near the resonance frequency with HR, as intended.

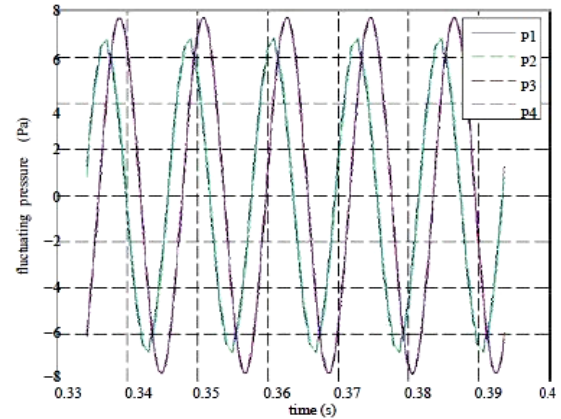


Fig. 9. Pressure fluctuations at location 1, 2, 3 and 4 for $u_{in}=17 \text{ m/s}$ at $f=84 \text{ Hz}$ without HR.

IV. CONCLUDING REMARKS

A computational model has been presented in this paper to predict the TL of a Helmholtz resonator placed parallel to the flow path. The predicted values of transmission loss are compared with the experimental results for validation. With sufficient care in choosing the numerical parameters such as proper differencing scheme and grid size, the predictions and experimental results show good agreement. Significant increase in flow rate (such as $Ma=0.1$) is shown to reduce the acoustic attenuation considerably, which is captured here both computationally and experimentally.

APPENDIX

Nomenclature

c	speed of sound
f	frequency
k	wave number ($=\omega/c$)
Ma	Mach number
p	pressure
$P(f)$	Fourier-transformed acoustic pressure
s	distance between microphones
t	time
u	velocity

Greek symbols

ω	angular frequency
----------	-------------------

Subscripts

i	incident
m	mean

r reflected

Abbreviations

FFT Fast Fourier Transform
 HR Helmholtz Resonator
 PISO Pressure-Implicit-Splitting-Operators
 rms Root Mean Square
 SPL Sound Pressure Level
 TL Transmission Loss

REFERENCES

- [1] A. Selamet and Z. L. Ji, "Circular asym-metric Helmholtz resonators," *Journal of the Acoustical Society of America*, vol. 107, no. 5, pp. 2360-2369, 2000.
- [2] A. Iqbal and A. Selamet, "A two-dimensional computational study of the flow effect on the acoustic behaviour of Helmholtz resonators," *International Journal of Vehicle Noise and Vibration*, vol. 6, no. 2-4, pp. 130-148, 2010.
- [3] J. S. Anderson, "The effect of an air flow on a single side branch Helmholtz resonator in a circular duct," *Journal of Sound and Vibration*, vol. 52, no. 3, pp. 423-431, 1977.
- [4] E. Selamet, A. Selamet, A. Iqbal, and H. Kim, "Effect of flow on Helmholtz resonator acoustics: A three-dimensional comput-ational study vs. experiments," SAE Paper, no. 2011-01-1521, SAE Noise and Vibration Conference, Grand Rapids, MI, May 17-19, 2011.
- [5] *Methodology, STAR-CD* (Version 4.12), Computer Software, CD-adapco, Melville, NY, 2009.
- [6] J. Y. Chung and D. A. Blaser, "Transfer function method of measuring in-duct acoustic properties," I. Theory, *Journal of the Acoustical Society of America*, vol. 68, no. 3, pp. 907-913, 1980.
- [7] J. Y. Chung and D. A. Blaser, "Transfer function method of measuring in-duct acoustic properties. II. Experiment," *Journal of the Acoustical Society of America*, vol. 68, no. 3, pp. 914-921, 1980.



Emel Selamet received her Ph.D. in Mechanical Engineering at University of Michigan in 1991; the M.S. in M.E. University of Michigan in 1986, the M.S. in Energy, M.E. Technical University of Istanbul, 1982. B.S. in. M. E. Technical University of Istanbul, 1980. She is a Research Scientist at Center for Automotive Center, The Ohio State University from 1997 to now. And she was the Research Fellow of University of Michigan from 1991 to 1995.